JOURNAL OF GUIDANCE, CONTROL, AND DYNAMICS
Vol. 22, No. 3, May–June 1999

Two-Timescale-Integration Method for Inverse Simulation

Giulio Avanzini* and Guido de Matteis†
Turin Polytechnic Institute, 10129 Turin, Italy
and
Luciano M. de Socio‡
University of Rome "La Sapienza," 00184 Rome, Italy

The integration method is extensively applied in the inverse simulation of aircraft motion where control inputs are determined once a maneuver or flight task is assigned. In many circumstances the presence of multiple timescales and right half-plane transmission zeros in aircraft dynamics introduces problems of accuracy and stability in the numerical algorithm. This paper presents a formulation for inverse simulation problems where the concept of timescale separation is merged into an integration technique and a constrained optimization method. Two subscale problems are solved separately for the slow and fast timescales and a numerical algorithm is devised that presents significant advantages in terms of numerical efficiency and robustness. The technique accounts for the issue of control saturation and lends itself to applications where the aircraft trajectory is given as a function of time. The results of the study show the improved performances of the technique in comparison with an integration method that is based on the local optimization concept.

Nomenclature

b	= wing span
C_l, C_m, C_n	= moment coefficients
C_T	= thrust coefficient
C_X, C_Y, C_Z	= force coefficients
$\bar{c}$	= mean aerodynamic chord
g	= gravity acceleration
$\boldsymbol{J}$	= Jacobian matrix
J_x, J_y, J_z	= moments of inertia
J_{xz}	= product of inertia
k_1, k_2	= curvature and torsion
$\boldsymbol{L}_{BI}, \boldsymbol{L}_{BW}, \boldsymbol{L}_{IW}, \boldsymbol{L}_{IF}$	= transformation matrices
M	= Mach number
m	= aircraft mass
Q	= dynamic pressure
$\boldsymbol{R}$	= $(R_N, R_E, R_D)^T$ inertial coordinate vector (North, East, and down, respectively)
s	= curvilinear abscissa
t	= time
$\boldsymbol{u}$	= control vector
V	= velocity modulus
$\boldsymbol{V}$	= velocity vector
$\boldsymbol{x}$	= state vector
$\boldsymbol{y}$	= output vector
α	= angle of attack
β	= sideslip angle
γ, μ, χ	= flight path, bank, and heading angles
Δt	= time interval of the slow dynamics
$\delta_A, \delta_E, \delta_R$	= aileron, elevator, and rudder angles
δ_T	= thrust level
δt	= time interval of the fast dynamics
δt_c	= time delay
$\delta\eta$	= time step for the numerical integration
ζ, ω_n	= damping coefficient and bandwidth of the filter
$\boldsymbol{\xi}$	= c.g. position in the Frenet triedron
ρ	= air density
$\boldsymbol{\Phi}$	= $(\phi, \theta, \psi)^T$ Euler angle vector
$\boldsymbol{\Omega}$	= $(p, q, r)^T$ angular velocity vector

Subscripts

C	= commanded
DES	= desired
F	= fast timescale
S	= slow timescale
s	= saturation

I. Introduction

THE purpose of this paper is to present a method for the inverse simulation that is based on the idea of timescale separation (TSS). The proposed technique is aimed at the realization of a new algorithm that produces significant improvements to existing methods for critical applications.

In recent times the inverse simulation of aircraft motion, where control inputs are to be determined for a prescribed flight maneuver or task, has counted a growing number of successful applications in flight mechanics. About a decade ago, a method of solution of the inverse problem, first approached in Ref. 1, found its application to the evaluation of the feasibility of prescribed maneuvers for a high performance aircraft model.[2] At the same time and in the wake of the first studies, Ref. 3 presented the inverse simulation as a method for quantifying the inherent agility of a helicopter. In this last case, once the time histories of the controls and the resulting states are determined for an assigned standard maneuver, the helicopter's performance is rated by a quadratic performance function of input and state variables. The same technique as in Ref. 3 is then extended[4] to predict the maximum maneuvering performance of a helicopter configuration during a specific mission. Both the issues of agility and maneuverability are considered in Ref. 4 and are represented, respectively, by the rate damping (or bandwidth) of the pitch and roll responses, and by the maximum load factor capability and the maximum pitch and roll rate capability. More recently inverse simulation is used to obtain a preliminary evaluation of the helicopter handling qualities[5] because it allows for the computation of the quickness values of the roll and control responses on assigned flight paths, and to investigate short timescale metrics of aircraft agility.[6] The technique in Ref. 6 is able to predict both the time history of the control inputs and the flight path that maximize the attainable value of a specified component of the agility vector.

A second, relevant field of application of inverse simulation is in the design of flight control systems. In this respect, Hess

Presented as Paper 97-0323 at the AIAA 35th Aerospace Sciences Meeting, Reno, NV, Jan. 6–9, 1997; received Aug. 6, 1998; revision received Dec. 14, 1998; accepted for publication Dec. 16, 1998.

*Research Fellow, Department of Aerospace Engineering. Member AIAA.
†Professor, Department of Aerospace Engineering; currently Department of Mechanics and Aeronautics, University of Rome "La Sapienza," 00184 Rome, Italy. Member AIAA.
‡Professor, Department of Mechanics and Aeronautics. Member AIAA.

and Gao[7] demonstrated that the inverse solution can be used to formulate task-driven bandwidth requirements for the design of stability augmentation systems. In a different framework, algorithms based on the solution of an inverse problem are developed to realize feedforward command generators for guidance controllers. This kind of application is proposed in Ref. 8 and is fully exploited in a recent study by Boyle and Chamitoff,[9] where the characteristics of an autonomous guidance system for an uninhabitated aerial vehicle (UAV) are reported. Here, the control system features a guidance subsection that generates local trajectory commands, an inverse simulation algorithm for the determinations of the input commands necessary to follow the specified flight path, and a linear quadratic tracking controller to account for nonmodeled dynamics and external disturbances. The performances of the controller appear to improve significantly when the values of the control variables calculated by inverse simulation are implemented in the reference command signal.

The guidance system reported in Ref. 9 is worth some further discussion. In fact, it represents a guidance controller where the determination of the control inputs and the implementation of a tracking control system are addressed separately to realize a system suitable for real-time applications. This technique may be regarded as a possible alternative to the design of real-time trajectory controllers based on TSS.[10–12] In these controllers, the guidance control algorithm relies on the solution of an inverse kinematic problem for the slow dynamics, and on a nonlinear inverse dynamics solution for the fast dynamics.

The issue of TSS is again considered in the present study, where two distinct, lower-order problems are formulated for the slow and fast timescales of the aircraft dynamics, and the control variables of the slow timescale are determined by solving an algebraic problem,[13] as will be shown in the sequel. The use of this procedure in inverse simulation eliminates unwanted effects that occur in the numerical accuracy and the stability of the solution algorithm when states associated to very different timescales are dealt with, and determines a significant improvement in terms of computational time. The proposed method that is, at least partially, founded on the integration approach[7] and on a local optimization technique[14] is particularly dedicated to those applications where the constrained output is a time-defined three-dimensional (four-dimensional) trajectory, because in these cases the presence of very slow and very fast states[11] can be a severe limitation for finding a realistic solution. Furthermore, a proper selection of the constraints and of a local performance index allows for the solution of problems where the trajectory is not fully defined. Finally, control amplitude and rate can be constrained to avoid the computation of unfeasible solutions because of the actuator saturation. In turn, the technique should eliminate the disadvantages of the other integration methods, while providing a fast, efficient, and robust algorithm for the inverse simulation.

In the following, after giving a concise report and a critical review on the state of the art in the field of the inverse simulation, the principal features of the proposed technique are presented in Sec. II. Then, the details of our method are given in Sec. III, and the applications are introduced and discussed in Sec. IV. In the same section the subsonic model for the F-16 fighter, which was considered throughout this work as a reference aircraft, is also briefly described.

II. Solving Inverse Simulation Problems

The algorithms proposed for the inverse simulation and adopted in one or the other of the applications cited in Sec. I fall into three distinct categories that correspond to techniques based on optimization, numerical differentiation, and numerical integration. The relevant aspects and the open problems associated with each of the three methods have been discussed in some detail in the literature. Our first objective here is to recall and compare briefly the various techniques and then to introduce a new approach to the integration method.

Optimization Methods

The formulation of the inverse problem as an optimization problem is proposed in Ref. 8 and more recently in Ref. 15, for the inverse simulation of the aileron roll of a A4D aircraft model. The study by Sentoh and Bryson[8] presents a linear quadratic technique for feedforward control design to solve a nominal problem, i.e., a problem where the number of controls (δ_A, δ_E, δ_R) is equal to the constrained outputs (p, y, z). The solution provides feasible and well-coordinated controls although, as a limitation, the assigned outputs cannot be realized with precision. This shortcoming occurs because the method is based on the minimization of the integral square deviation of the calculated trajectory from the prescribed one under constraints on the control variables.

A different technique[15] is based on a variational approach where a general optimization problem is solved with equality constraints enforced on the output variables. In redundant problems, where the number of controls is greater than the number of the output variables, a proper selection of the performance index and of the constraints is shown to determine well-coordinated responses with reduced control deflections. A significant advantage of this last technique is that neither the differentiation in time of the path constraints as in the differentiation methods nor the partial differentiation of the output variables with respect to the control variables as in the integration methods is required. In Ref. 15 the governing set of equations of the system is in the form

$$\dot{\boldsymbol{x}} = \boldsymbol{f}(\boldsymbol{x}, \boldsymbol{u}, t), \qquad \boldsymbol{x} \in \mathcal{R}^5, \qquad \boldsymbol{u} \in \mathcal{R}^3 \tag{1}$$

and the Jacobian matrix $\partial \boldsymbol{f}/\partial \boldsymbol{x}$ is analytically expressed for a simple A4D model where the forward velocity is constant, and a linear aerodynamic model and quasilinear kinematics are considered. When more complete aircraft models featuring nonlinear aerodynamics and/or control and stability augmentation system, or helicopter models are dealt with, the analytical expression of $\partial \boldsymbol{f}/\partial \boldsymbol{x}$ introduces such a significant overhead as to inhibit the applicability of the technique.

Differentiation Methods

Techniques based on the differentiation approach reduce the set of differential equations of motion to an algebraic system by numerical differentiation of the assigned trajectory constraints. The solution algorithm is fast enough from the computational point of view so that real-time solutions are provided that are suitable for onboard implementation. Relevant contributions where this approach is used are those presented in Refs. 1, 3, 5, 9, and in the study by Rutheford and Thomson,[16] where a detailed examination of the method is presented in comparison with the integration techniques. In Ref. 16 it is shown that the major limitation of the differentiation approach is the coupling between the mathematical model and the inverse solution algorithm that needs significant restructuring for any modification of the vehicle model. Also, it has been highlighted[8,15] that problems may arise in some applications where the assigned output is hardly achievable, in the form of infeasible or poorly coordinated solutions with unacceptable secondary outputs. Finally, as a further and maybe essential drawback, we observe that the method is not suitable for the solution of redundant problems.

Integration Methods

The integration approach relies on the numerical integration of the equations of motion for a sequence of time intervals δt. Each control variable, which is usually assumed constant within the time step δt, is modified until, at the end of the same interval, the output variables are brought to the desired value. The same procedure is then repeated step by step for the whole duration of the considered maneuver. Among others we cite here the earlier applications of the method[17,7] and two papers[14,16] where some improvements to the basic approach are provided. Probably the major advantage of this method lies in its generality because different vehicle models can be implemented without modifications of the inversion algorithm. Furthermore, the technique can deal efficiently with redundant problems through either the concept of generalized inverse matrix[17] or, as reported in Ref. 14, by a local optimization method where a suitable cost function is minimized to tailor the inverse solution according to desired prerequisites. Also, using the latter procedure, the controls and states can be bounded, respectively, to keep the problem of saturation under control and limit the variation of secondary outputs.

On the other hand, the integration methods suffer from some limitations and some unresolved problems that are mainly related to

the important issue of numerical stability. In this respect the conclusions presented in Refs. 18 and 16 are of great interest. In summary, a first aspect is related to the poor accuracy of solutions that are obtained by using a too small discretization interval δt, because of the errors carried by uncontrolled state variables.[18] Then, and probably more important, accuracy and stability problems may arise as a result of the evaluation of the Jacobian matrix $\boldsymbol{J} = \partial \boldsymbol{y}/\partial \boldsymbol{u}$. The elements of $\boldsymbol{J}$ depend on dynamic states and consequently their numerical approximation, which is computed by simulation at each time step, is significantly affected by the length of the discretization interval. This is by no means a problem of numerical accuracy in the classical sense but rather a natural consequence of the presence of multiple timescales in the system dynamics. In this respect, the effect of δt on the global stability of the integration method is examined in Ref. 19, where a discrete model of the algorithm of Ref. 17 is derived. One can immediately observe that the correct evaluation of the Jacobian may represent a subtle task when nonminimum-phase systems are taken into consideration. In aircraft and helicopter response, right half-plane transmission zeros are present because of the coupling between the generation of control forces and moments that are associated, respectively, to slow and fast dynamics.

In Ref. 16 it is emphasized that δt cannot be too small to allow the transient dynamics of the system to settle and hence to realize a good prediction of the effect of controls on the longer term dynamics. To the same goal, in Ref. 14, the desired value of the output is imposed with a delay δt_c such that, as far as an accurate estimate of the Jacobian matrix $\boldsymbol{J}$ is concerned, the short-period dynamics of the aircraft subside. As a further observation, it is shown in Ref. 16 that the unstable oscillations in the inverse solutions are completely eliminated provided that the components of the c.g. inertial acceleration are given as outputs instead of the Cartesian coordinates. It is evident that removing very slow states from the inverse problem leads to a better quality of the results.

We can now recognize that the advantages of an integral technique will be further exploited when the shortcomings associated to the multiple scales and right half-plane zeros in the aircraft response are properly dealt with. Here the approach based on TSS is applied to the solution of inverse problems and we retain the basic assumption, already discussed in a number of studies,[11,12] that the control variables of the fast dynamics and the components of the angular velocity have a negligible effect on the slow dynamics.

The TSS concept is adopted in a recent work,[13] where use is made of the intrinsic or Frenet coordinate system to obtain a fast and stable forward integration procedure for the aircraft equations of motion. In the present study, once the c.g. motion is decoupled from the attitude dynamics over a time interval of the order of the long timescale, the slow, trajectory-related variables are expressed by a proper expansion of the flight path in the Frenet triad to deal with an algebraic problem for the slow dynamics.[13] In this way two uncoupled inverse subproblems are formulated, the first of which, on the slow timescale, is algebraic and redundant, whereas the second, for the fast timescale, attitude variables is dynamic and nominal. In both cases, the solution, in terms of unknown controls or pseudocontrols to be determined, is provided by the constrained optimization method of Ref. 14. In particular, on the slow timescale one evaluates the thrust level δ_T and, as pseudocontrols, the angle of attack $\bar{\alpha}$, the sideslip angle $\bar{\beta}$, and the bank angle of the lift vector $\bar{\mu}$, whereas the aerodynamic control angles δ_E, δ_A, and δ_R are the unknowns of the fast timescale problem.

III. Analysis

In this section we present the method for the solution of the inverse problem on two timescales. Considering zero ambient wind, the flat-Earth equations of motions for the aircraft c.g. are written in wind axes $\mathcal{F}_W$, whereas, as usual, the equations for the attitude dynamics are in a body-fixed reference frame $\mathcal{F}_B$.

Slow Timescale

The state and control vectors for the slow dynamics are, respectively, $\boldsymbol{x}_S = (V, \chi, \gamma, \boldsymbol{R})^T$ and $\boldsymbol{u}_S = (\bar{\alpha}, \bar{\beta}, \bar{\mu}, \delta_T)^T$ where $\bar{\alpha}$, $\bar{\beta}$, and $\bar{\mu}$ can be interpreted as pseudocontrols. The point mass equations for the c.g. dynamics and the kinematic relations for the c.g. coordinates in the inertial frame are as follows:

$$\begin{aligned}
\dot{V} &= \frac{QS}{m}[(C_T + C_X)\cos\bar{\alpha}\cos\bar{\beta} + C_Y \sin\bar{\beta} \\
&\quad + C_Z \sin\bar{\alpha}\cos\bar{\beta}] - g\sin\gamma \\
\dot{\chi} &= \frac{QS}{mV\cos\gamma}\{[-(C_T + C_X)\cos\bar{\alpha}\sin\bar{\beta} \\
&\quad + C_Y \cos\bar{\beta} - C_Z \sin\bar{\alpha}\sin\bar{\beta}]\cos\bar{\mu} \\
&\quad + [(C_T + C_X)\sin\bar{\alpha} - C_Z\cos\bar{\alpha}]\sin\bar{\mu}\} \\
\dot{\gamma} &= \frac{QS}{mV}\{[(C_T + C_X)\cos\bar{\alpha}\sin\bar{\beta} - C_Y\cos\bar{\beta} \\
&\quad + C_Z \sin\bar{\alpha}\sin\bar{\beta}]\sin\bar{\mu} + [(C_T + C_X)\sin\bar{\alpha} \\
&\quad - C_Z\cos\bar{\alpha}]\cos\bar{\mu}\} - \frac{g}{V}\cos\gamma
\end{aligned} \tag{2}$$

$$\dot{R}_N = V\cos\chi\cos\gamma, \qquad \dot{R}_E = V\sin\chi\cos\gamma$$
$$\dot{R}_D = -V\sin\gamma \tag{3}$$

where $Q = 0.5\rho(R_D)V^2$ and $C_T = C_T(V, R_D, \delta_T)$. Unless a simplified form of the polar curve of the aircraft is assumed, the coefficients C_X, C_Y, and C_Z are usually given in tabular form as functions of α and β. If the inertial coordinates $\boldsymbol{R}_{\mathrm{DES}}(t)$ of a desired trajectory are assigned as a function of time, then the elements of the constrained output vector $\boldsymbol{y}_{S_{\mathrm{DES}}} = [V(t), \chi(t), \gamma(t)]^T_{\mathrm{DES}}$ are expressed as

$$V(t) = |\dot{\boldsymbol{R}}|, \qquad \chi(t) = \tan^{-1}(\dot{R}_E/\dot{R}_N)$$
$$\gamma(t) = -\sin^{-1}(\dot{R}_D/V) \tag{4}$$

In other circumstances the four-dimensional trajectory may be provided in terms of the magnitude and direction of the velocity vector vs time so that the desired values of V, γ, and χ are already known and Eqs. (4) are not used.

As was said previously in this paper, a way to evaluate the coordinates in a direct algebraic form is to make use of the intrinsic coordinates. Let us recall that the Frenet or intrinsic reference frame $\mathcal{F}_F$ is a triad fixed to the trajectory, with unit vectors in each point of the curve that are directed along the local tangent, radius of curvature, and binormal. Consider the position of $\mathcal{F}_F$ fixed at a given time t_0 and let $s(t - t_0)$ be the curvilinear coordinate along the c.g. trajectory with $s(0) = 0$. In this set of axes the flight path can be approximated by a cubic helix, according to the expansion[13]

$$\boldsymbol{\xi}(s) = \begin{bmatrix} s - \dfrac{s^3\left(k_1^2\right)_0}{3!} \\ \dfrac{s^2(k_1)_0}{2!} + \dfrac{s^3(k_1')_0}{3!} \\ \dfrac{s^3(k_1k_2)_0}{3!} \end{bmatrix} \tag{5}$$

which is accurate to the third order in s and where the superscript $(')$ stays for derivative with respect to s. Furthermore, to the same order of accuracy in t, one has

$$s(t - t_0) = V_0(t - t_0) + \frac{\dot{V}_0(t - t_0)^2}{2!} + \frac{\ddot{V}_0(t - t_0)^3}{3!} \tag{6}$$

The expressions of the curvature and torsion, namely k_1 and k_2, are[20]

$$k_1 = (1/V^2)(|\ddot{\boldsymbol{R}}|^2 - \dot{V}^2)^{\frac{1}{2}} \tag{7}$$

$$k_2 = \frac{\det\{\dot{\boldsymbol{R}}, \ddot{\boldsymbol{R}}, \dddot{\boldsymbol{R}}\}}{V^2(|\ddot{\boldsymbol{R}}|^2 - \dot{V}^2)} \tag{8}$$

and $k_1' = \dot{k}_1/V$. After introducing Eq. (6) in Eq. (5) and taking into account Eqs. (7) and (8), a third-order accurate approximation for $\boldsymbol{R}(t)$ can be obtained

$$\boldsymbol{R}(t) = \boldsymbol{R}(t_0) + \boldsymbol{L}_{IF}(t_0)\boldsymbol{\xi}(t - t_0) \tag{9}$$

where the transformation matrix $\boldsymbol{L}_{IF}$ from the Frenet frame to the inertial frame is expressed as

$$\boldsymbol{L}_{IF}(t_0) = (\dot{\boldsymbol{R}}/V, \boldsymbol{n}/|\boldsymbol{n}|, \tilde{\boldsymbol{R}}\boldsymbol{n}/V|\boldsymbol{n}|)_0 \tag{10}$$

In Eq. (10) $\boldsymbol{n} = \ddot{\boldsymbol{R}} - \dot{\boldsymbol{R}}\dot{V}/V$ and $\tilde{\boldsymbol{R}}\boldsymbol{n}$ is the matrix equivalent of vector product. It is worth remarking that in straight-line flight $k_1 = 0$, $\boldsymbol{n} = 0$, and k_2 is undetermined. This apparent disadvantage of using the Frenet triad is easily eliminated. The aforementioned circumstance corresponds, in terms of constrained output, to $\dot{\chi} = \dot{\gamma} = 0$, and Eq. (9) still holds in the form

$$\boldsymbol{R}(t) = \boldsymbol{R}(t_0) + (\dot{\boldsymbol{R}}/V)_0\, s(t - t_0) \tag{11}$$

because all of the quantities to be evaluated are in the direction of the local tangent.

Using Eq. (9) an estimate of the aircraft position at time t is obtained once the first, second, and third derivatives of $\boldsymbol{R}$ are evaluated at t_0. In this respect, $\dot{\boldsymbol{R}}_0$ is immediately determined by Eqs. (3), and $\ddot{\boldsymbol{R}}_0$ is evaluated after Eqs. (3) are analytically differentiated and Eqs. (2) are used to express $\dot{V}$, $\dot{\chi}$, and $\dot{\gamma}$. Finally, $\dddot{\boldsymbol{R}}_0$ is written as

$$\dddot{\boldsymbol{R}}_0 = \left.\frac{\partial \ddot{\boldsymbol{R}}}{\partial \boldsymbol{x}_S}\right|_0 \dot{\boldsymbol{x}}_S(t_0) + \left.\frac{\partial \ddot{\boldsymbol{R}}}{\partial \boldsymbol{u}_S}\right|_0 \dot{\boldsymbol{u}}_S(t_0) \tag{12}$$

where $\partial\ddot{\boldsymbol{R}}/\partial\boldsymbol{x}_S$ and $\partial\ddot{\boldsymbol{R}}/\partial\boldsymbol{u}_S$ are numerically evaluated by centered finite differences, $\dot{\boldsymbol{x}}_S$ is given by Eqs. (2) and (3), and provided that $\dot{\boldsymbol{u}}_S(t)$ is also available. At this point, being $\dot{\boldsymbol{R}}(t) = \boldsymbol{L}_{IF}(t_0)\dot{\boldsymbol{\xi}}(t - t_0)$ as obtained by differentiation of Eq. (9) with respect to t [or $\dot{\boldsymbol{R}}(t) = (\dot{\boldsymbol{R}}/V)_0\, \dot{s}(t - t_0)$ from Eq. (11) for straight-line flight], the slow states at time t are determined according to Eqs. (4), and, in concise form, we can write

$$\boldsymbol{x}_S(t) = \boldsymbol{F}[\boldsymbol{x}_S(t_0), \boldsymbol{u}_S(t_0), \dot{\boldsymbol{u}}_S(t_0), t] \tag{13}$$

An algorithm based on the preceding expansions is now presented. Let t_{i-1} and t_i be the bounds of the ith discretization interval, the duration of which is Δt, and let the state $\boldsymbol{x}_S(t_k)$ and the control $\boldsymbol{u}_S(t_{k+1/2})$ be already known for $1 \le k \le i - 1$. Also, note that in the slow-time problem the state is assigned in the nodes t_i, whereas the values of the controls are evaluated in the semi-intervals. We have to determine the control vector $\boldsymbol{u}_S^{(*)}(t_{i+1/2})$ that realizes the desired value of the output $\boldsymbol{y}_S$ at time t_{i+1}. To this end, a suitable guess $\boldsymbol{u}_S^{(0)}(t_{i+1/2})$ is considered, and $\boldsymbol{u}_S(t_i)$ and $\dot{\boldsymbol{u}}_S(t_i)$ are expressed as

$$\begin{aligned} \boldsymbol{u}_S(t_i) &= \frac{\boldsymbol{u}_S(t_{i-1/2}) + \boldsymbol{u}_S^{(0)}(t_{i+1/2})}{2} \\ \dot{\boldsymbol{u}}_S(t_i) &= \frac{\boldsymbol{u}_S^{(0)}(t_{i+1/2}) - \boldsymbol{u}_S(t_{i-1/2})}{\Delta t} \end{aligned} \tag{14}$$

Then, use is made of Eqs. (5), (7), (8), and (10), now written for $t_0 = t_i$, to obtain from Eq. (9) a third-order accurate approximation of the output vector at the time t_{i+1} and we may thus write

$$\begin{aligned} \boldsymbol{y}_S(t_{i+1}) &= \boldsymbol{G}[\boldsymbol{x}_S(t_{i+1})] \\ &= \boldsymbol{G}\left\{\boldsymbol{F}\left[\boldsymbol{x}_S(t_i), \boldsymbol{u}_S(t_{i-1/2}), \boldsymbol{u}_S^{(0)}(t_{i+1/2}), t_{i+1}\right]\right\} \end{aligned} \tag{15}$$

Since the slow timescale problem expressed by Eq. (15) can be considered as an inverse problem when $\boldsymbol{u}_S^{(*)}(t_{i+1/2})$ is to be determined such that the constraint $\boldsymbol{y}_S(t_{i+1}) = \boldsymbol{y}_{S_{\mathrm{DES}}}(t_{i+1})$ is satisfied, then the solution is obtained by a constrained optimization algorithm. In fact, the set of Eq. (15) is algebraic and has one degree of redundancy as $\boldsymbol{y}_S \in R^3$ and $\boldsymbol{u}_S \in R^4$. The redundancy is exploited either by imposing a further constraint, such as a zero sideslip angle, or by introducing a local penalty index to realize some desirable properties for the resulting maneuver. In this latter case, for instance, we can obtain minimum thrust variation, or minimum β when a flight with zero sideslip is not feasible.

At the end of this section we should recall that the pseudocontrols $\bar{\alpha}$, $\bar{\beta}$, and $\bar{\mu}$ that have just been determined define the assigned output variables for the fast timescale problem. In this respect their expressions in the time interval $[t_{i-1}; t_i]$ must be evaluated in such a way to preserve their continuity and the continuity of their first derivatives at the bounds of the same interval. Therefore, by using the values of $\boldsymbol{u}_S$ and $\dot{\boldsymbol{u}}_S$ at $t = t_{i-1}$ and t_i as computed according to the form of Eqs. (14), the control vector is interpolated by a third-order polynomial in the interval $[t_{i-1}; t_i]$ to obtain a control law $\boldsymbol{u}_S(t)$ of class C^1.

Fast Timescale

In the fast timescale the state vector is $\boldsymbol{x}_F = (\boldsymbol{\Omega}, \boldsymbol{\Phi})^T$ and the control vector is $\boldsymbol{u}_F = (\delta_A, \delta_E, \delta_R)^T$. The equations governing the short-term dynamics can be expressed as follows:

$$\dot{\boldsymbol{\Omega}} = \begin{bmatrix} \dfrac{A_p J_z + A_r J_{xz}}{J_x J_z - J_{xz}^2} \\ \dfrac{\left[J_{xz}(r^2 - p^2) + (J_z - J_x)pr + QS\bar{c}C_m\right]}{J_y} \\ \dfrac{A_r J_x + A_p J_{xz}}{J_x J_z - J_{xz}^2} \end{bmatrix} \tag{16}$$

$$\dot{\boldsymbol{\Phi}} = \begin{bmatrix} 1 & \sin\phi\tan\theta & \cos\phi\tan\theta \\ 0 & \cos\phi & -\sin\phi \\ 0 & \sin\phi\sec\theta & \cos\phi\sec\theta \end{bmatrix} \boldsymbol{\Omega} \tag{17}$$

where

$$A_p = J_{xz}pq + (J_y - J_z)qr + QSbC_l$$

$$A_r = -J_{xz}qr + (J_x - J_y)pq + QSbC_n$$

The aerodynamic moment coefficients C_l, C_m, and C_n depend on $\bar{\alpha}$, $\bar{\beta}$, $\boldsymbol{\Omega}$, and $\boldsymbol{u}_F$.

Now the problem is finding the control law that realizes the desired variation of the angle of attack $\bar{\alpha}$, the sideslip angle $\bar{\beta}$, and the bank angle $\bar{\mu}$, as supplied by the algorithm for the inverse problem of the slow timescale. The variables to be tracked are the attitude angles $(\phi, \theta, \psi)_{\mathrm{DES}} = \boldsymbol{\Phi}_{\mathrm{DES}}^T$, that are determined by the equation

$$\boldsymbol{L}_{BI}(\boldsymbol{\Phi}_{\mathrm{DES}}) = \boldsymbol{L}_{BW}(\bar{\alpha}, -\bar{\beta})\boldsymbol{L}_{WI}(\bar{\mu}, \gamma, \chi) \tag{18}$$

when we take $\bar{\alpha}$, $\bar{\beta}$, $\bar{\mu}$ from $\boldsymbol{u}_S$ and γ, χ as obtained from the integration of Eqs. (2).

At this point we observe that $\boldsymbol{\Phi}_{\mathrm{DES}}$ has the same C^1 class of continuity as $\boldsymbol{u}_S$. Therefore, to avoid a discontinuity on $\dot{\boldsymbol{\Omega}}$ (function of $\ddot{\boldsymbol{\Phi}}_{\mathrm{DES}}$) at the bounds of the interval $[t_{i-1}; t_i]$ that would lead to a noncontinuous variation of $\boldsymbol{u}_F$, the commanded attitude $\boldsymbol{\Phi}_C$ is given the following dynamics:

$$\ddot{\boldsymbol{\Phi}}_C + 2\omega_n\zeta\dot{\boldsymbol{\Phi}}_C + \omega_n^2(\boldsymbol{\Phi}_C - \boldsymbol{\Phi}_{\mathrm{DES}}) = 0 \tag{19}$$

where a bandwidth ω_n of 10 rad s^{-1} has been selected as suggested in Ref. 11, and the damping coefficient is $\zeta = 0.9$. When Eq. (19) is used, the resulting control law $\boldsymbol{u}_F(t)$ is well behaved.

In the fast timescale we have a nominal problem because the output $\boldsymbol{y}_{F_{\mathrm{DES}}} = \boldsymbol{\Phi}_C \in \mathcal{R}^3$ is to be realized by the three moment-generating controls δ_A, δ_E, and δ_R. The inverse solution is obtained by the integration technique reported in Ref. 14 that relies on the same constrained optimization algorithm adopted in the slow timescale. Although the use of constrained optimization for solving a nominal problem may appear as a source of unnecessary complexity from the computational point of view, it has the advantage that some very meaningful inequality constraints can be enforced. For instance, in those maneuvers where control saturation may occur, the code pursues solutions that minimize the maximum deviation from the desired values of the output variables.

Here we consider piecewise constant controls in the interval $\delta t = \Delta t/N$, where N is the number of subintervals in which $\boldsymbol{u}_F$ is to be calculated, and we remark that the output $\boldsymbol{y}_{F_{\mathrm{DES}}}$ is tracked with zero delay because only short-term dynamics are present.

IV. Results and Discussion

The proposed technique is hereafter applied to the inverse simulation of a few significant maneuvers of a simplified model of the F-16 fighter aircraft, as described in detail in Ref. 21. The model has a Mach number limit equal to 0.6 and the aerodynamic coefficients are provided in tabular form as functions of α, β, p, q, r and the control angles. In this study, the dependence of the force coefficients on the angular velocity components and on the fast timescale control variables δ_E, δ_A, and δ_R has been neglected according to the TSS approach.[11] As a further simplification, the engine dynamics has not been taken into consideration. Because the aircraft stability and control augmentation system (SCAS) is not featured in the model and the F-16 has a slightly negative static margin, the c.g. has been moved forward to realize the desired level of stability with $x_{cg} = 0.30\bar{c}$. Nevertheless, results obtained with the c.g. in the nominal position at $0.35\bar{c}$, and therefore with a statically unstable aircraft model, showed negligible differences from those corresponding to the forward c.g. location. In all of the cases reported here, a time step $\delta\eta = \frac{1}{64}$ s was used for the forward integration of the complete set of Eqs. (2), (3), (16), and (17) by a fourth-order Runge-Kutta routine.

As a first application we consider an altitude variation of the model aircraft to be realized at constant speed in the vertical plane. The results for this simple maneuver provide some insight into the effects of filtering the attitude commands in the fast-time scale. The assigned variables are

$$R_{D_{\mathrm{DES}}} = 0, \qquad t \le 2 \text{ s}$$

$$R_{D_{\mathrm{DES}}} = -\tfrac{15}{16}\{\cos[3\pi(t-2)/5] - 9\cos[\pi(t-2)/5] + 8\} \text{ m} \qquad 2 < t < 7 \text{ s}$$

$$R_{D_{\mathrm{DES}}} = -15 \text{ m}, \qquad t \ge 7 \text{ s}$$

$$V_{\mathrm{DES}} = 76.2 \text{ ms}^{-1}, \qquad t \ge 0 \text{ s}$$

The problem is nominal in the slow timescale with two unknowns, $\bar{\alpha}$ and δ_T, and two constraints. The time length of the maneuver is equal to 10 s and the values of the time intervals Δt and δt are $\frac{1}{4}$ and $\frac{1}{32}$ s, respectively. Figure 1 shows the variation of meaningful variables and of the slow (δ_T) and fast (δ_E) controls. In particular, the dashed and continuous lines in Fig. 1a show, respectively, $R_{D_{\mathrm{DES}}}$ and the values of R_D actually achieved under the control laws that result from the inverse simulation. Figure 1b shows the pseudocontrol $\bar{\alpha}$ and the desired pitch angle θ_{DES} (dashed lines) together with the values of α and θ computed by the forward simulation. Figures 1c and 1d report, respectively, δ_T and δ_E vs time. The latter figure shows how the required continuity of the fast control is realized by the second-order filter of Eq. (19), a further effect of which is the small lag observable in the R_D, α, and θ plots. The noncontinuous variation of δ_E that would occur in the absence of the filter is also reported in the same figure. The maximum difference between the desired and the achieved velocity is as low as 0.5%.

The second maneuver is a sequence of three turns in the horizontal plane to be realized at constant speed in a time interval of 20 s. The desired variation of $R_E(t)$ is

$$R_{E_{\mathrm{DES}}} = 200\{1 - [(t-11)/10]^2\}^4 \text{ m}, \qquad 1 < t < 21 \text{ s}$$

$$R_{E_{\mathrm{DES}}} = 0 \text{ m}, \qquad t \le 1 \text{ s} \quad t \ge 21 \text{ s}$$

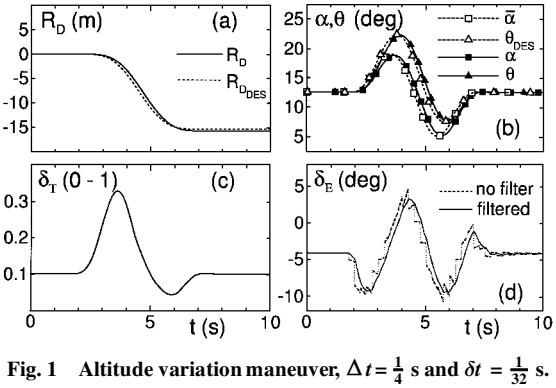

Fig. 1 Altitude variation maneuver, $\Delta t = \frac{1}{4}$ s and $\delta t = \frac{1}{32}$ s.

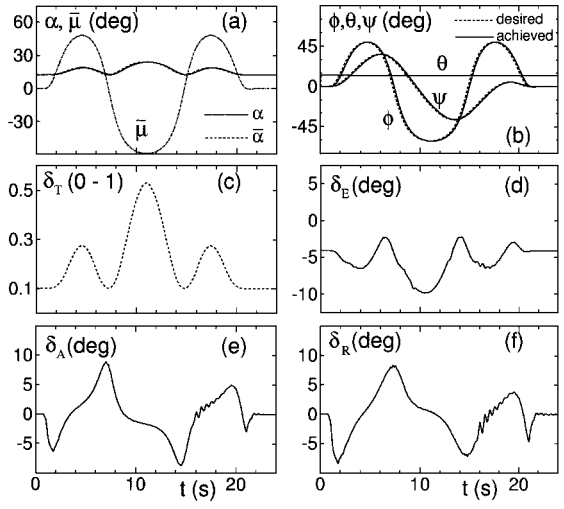

Fig. 2 Sequence of three turns in the horizontal plane, $\Delta t = \frac{1}{4}$ s and $\delta t = \frac{1}{32}$ s.

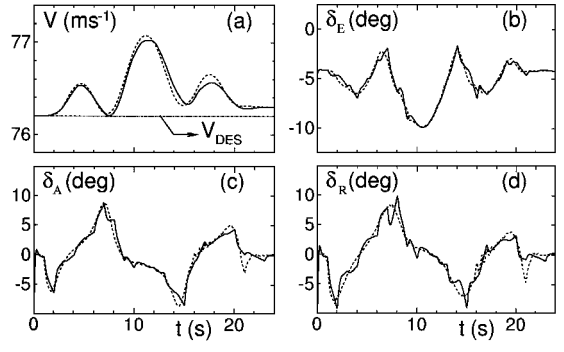

Fig. 3 Sequence of turns in the horizontal plane, effect of the time interval of the slow dynamics $\delta t = \frac{1}{32}$ s: ——, $\Delta t = 1$ s, and – – –, $\Delta t = \frac{1}{4}$ s.

The trajectory is assigned in terms of V, χ, and γ as

$$\chi_{\mathrm{DES}} = \sin^{-1}\left(\frac{\dot{R}_{E_{\mathrm{DES}}}}{V_{\mathrm{DES}}}\right), \qquad V_{\mathrm{DES}} = 76.2 \text{ ms}^{-1}, \qquad \gamma_{\mathrm{DES}} = 0$$

The slow timescale problem is now redundant because we have three constrained variables and four unknown quantities in $\boldsymbol{u}_S$. Therefore a local penalty index is defined as $S = \bar{\beta}^2$ to obtain solutions where the sideslip angle is kept to a minimum. The results for $\Delta t = \frac{1}{4}$ s and $\delta t = \frac{1}{32}$ s are reported in Fig. 2. The pseudocontrols $\bar{\alpha}$ and $\bar{\mu}$ (Fig. 2a) are given together with the achieved values of α as obtained by the forward integration of the complete set of governing equations once the control variables have been determined. The achieved slow states V, γ, and χ are very close to the desired values with differences lower than 2%. Next, the attitude angles are shown in Fig. 2b, the only difference between the commanded and achieved values being a small delay because of the filter. Finally, the control angles are shown in Figs. 2c–2f. Note that the low amplitude oscillations that are present in the δ_E, δ_A, and δ_R plots for $16 \le t \le 18$ s are completely eliminated by using $\Delta t = \frac{1}{8}$ s.

Figure 3 reports the effect of the time interval of the slow timescale Δt. In Fig. 3a the plots of the achieved V are presented for $\Delta t = \frac{1}{4}$ s (dashed lines) and $\Delta t = 1$ s (continuous lines). The computed values of the R_E coordinate for the two time intervals (not shown in the figure) are substantially indistinguishable from the desired R_E, even though a small delay (shorter than 0.25 s), because of the filtering of the commanded attitude angles, is apparent. Finally, in Figs. 3b–3d we have the fast timescale controls. We observe that although the control variables present differences as high as several degrees (Figs. 3c and 3d), the solutions of the forward simulation in the two cases appear quite similar, and the differences with the desired values are smaller as the timescale of the considered output is slower. For instance, we see in Fig. 3a a maximum variation of 1.5% on V.

Table 1 CPU time (in seconds) for the timescale separation method

Δt, s	RK steps	$\delta t = \frac{1}{4}$ s	$\delta t = \frac{1}{8}$ s	$\delta t = \frac{1}{32}$ s
1	64	16.7	15.7	17.2
$\frac{1}{2}$	32	16.8	16.1	17.4
$\frac{1}{4}$	16	17.0	16.5	17.5
$\frac{1}{8}$	8	——	16.9	17.7
$\frac{1}{16}$	4	——	——	18.6
$\frac{1}{32}$	2	——	——	20.1

Table 2 CPU time (in seconds) for the local optimization technique[14]

δt_c, s	RK steps	$\delta t = \frac{1}{4}$ s	$\delta t = \frac{1}{8}$ s	$\delta t = \frac{1}{32}$ s
$\frac{3}{4}$	48	58.4	111.9	430.1
$\frac{1}{2}$	32	37.3	74.0	284.0
$\frac{1}{4}$	16	——	39.3	151.3
$\frac{1}{8}$	8	——	——	80.1
$\frac{1}{16}$	4	——	——	43.6

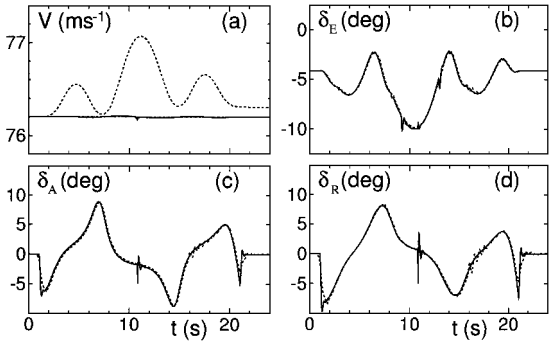

Fig. 4 Sequence of turns in the horizontal plane, effect of the inverse simulation technique: ——, local optimization (Ref. 14), $\delta t_c = \frac{1}{8}$ s, and – – –, timescale separation, $\Delta t = \frac{1}{4}$ s.

In Table 1 the CPU time required on a Pentium 200 MHz with MMX for the inverse solutions of the preceding maneuver is reported. Reference to the computer time for solving the same problem by the local optimization technique[14] is provided in Table 2. In the application of the method in Ref. 14, the same $\delta\eta = \frac{1}{64}$ s for the Runge-Kutta algorithm was used, and we recall that the discretization interval corresponds to the fast timescale interval δt and that the delay δt_c allows for the fast dynamics to subside before the constraints are enforced. The first remark on the results of Table 1 regards the moderate effect of the time length of the slow timescale interval Δt. As we said, the slow timescale inverse problem is an algebraic one, the solution of which takes very limited computational time. For any value of Δt, the minimum CPU time occurs at an intermediate value of δt, i.e., $\delta t = \frac{1}{8}$ s. This fact can be explained when the effect of the initial guess on the convergence of the inversion algorithm at each step in the fast timescale is taken into account. In fact, the converged values of the fast control variables at any step are used as first guesses for the inverse solution at the next step. Therefore, a shorter δt produces better initial guesses that in turn determine a reduction of the number of iterations necessary to obtain a converged solution. On the other hand, when δt becomes very small, the total CPU time is increased because of the much higher number of steps.

As for the results obtained using the local optimization method,[14] we observe that the CPU time is larger at least by a factor of 2.5. Furthermore, it has to be pointed out that the solutions with shorter delays present marked oscillations in the control angles. For instance, the control laws obtained using the shortest time delay, i.e., $\delta t_c = \frac{1}{16}$ s (CPU time equal to 43.6 s), show oscillations having such a high amplitude that the aerodynamic controls saturate. In this respect, Fig. 4 reports some comparisons of the inverse solutions as computed by the present technique (dashed lines, $\Delta t = \frac{1}{4}$ s, $\delta t = \frac{1}{32}$ s, CPU time equal to 17.5 s) and the method of Ref. 14 (continuous line, $\delta t_c = \frac{1}{8}$ s, $\delta t = \frac{1}{32}$ s, CPU time equal to 80.1 s). The amplitude of the oscillations on δ_A and δ_R, visible in Figs. 5c and 5d for the local optimization technique[14] (continuous line), can be significantly reduced provided that a delay δt_c of at least $\frac{1}{4}$ s is used. In this latter circumstance the CPU time grows as high as 151.3 s and, in comparison, the TSS method is faster by a factor of 8.6.

To illustrate how the present method deals with control saturation we determine the control laws to realize the following maneuver:

$$R_{E_{\mathrm{DES}}} = 318\{1 - [(t-8)/7]^2\}^4 \text{ m}, \qquad 1 < t < 15 \text{ s}$$
$$R_{E_{\mathrm{DES}}} = 0 \text{ m}, \qquad t \le 1 \text{ s}, \quad t \ge 15 \text{ s}$$

with $V_{\mathrm{DES}} = 152.4$ ms^{-1} and $\gamma_{\mathrm{DES}} = 0$, which again represents a sequence of turns at constant speed and altitude. During the maneuver, control saturation occurs because of amplitude and rate limited actuators. In particular, the rate limit ($\dot{\delta}_s$) is 60, 50, and 120 deg s^{-1} for elevator, ailerons, and rudder, respectively.[22] The upper and lower amplitude limits (δ_{s_u}, δ_{s_l}) are ±25, ±21.5, and ±30 deg for δ_E, δ_A, and δ_R, respectively. Therefore, the constraints on the control angles are given by expressing their maximum ($\delta_{\max}$) and minimum value ($\delta_{\min}$) in the following form for the jth interval of constant control, with $1 \le j \le N$:

$$(\delta_j)_{\max} = \min\left[\delta_{s_u};\ \delta_{j-1} + \dot{\delta}_s\,\delta t\right]$$
$$(\delta_j)_{\min} = \max\left[\delta_{s_l};\ \delta_{j-1} - \dot{\delta}_s\,\delta t\right]$$

We observe in Fig. 5, where the results obtained in the absence of rate and amplitude limiting are also reported for comparison, that rate saturation occurs at $t = 5.6$ and 10.8 s for the ailerons and about 0.2 s later for the rudder. The sharp variation of the rudder angle is because of the request for a larger roll moment when the aileron angle is rate limited so as to minimize the mean square deviation of the Euler angles from the prescribed values.

The final considered maneuver is a 360-deg aileron roll to be executed on a straight trajectory and maintaining a constant speed. This case presents some peculiar aspects for the application of our two timescale method because, as we said in Sec. III, we have $k_1 = 0$ and k_2 undetermined. Of course the law $\mu(t)$ is also to be assigned to have the aircraft roll. Also, when the maneuver is carried out rather slowly as in the present circumstance where the roll takes 11 s, not negligible lateral forces are to be generated during the vehicle rotation to sustain the desired flight path. Therefore the full control of the slow and fast dynamics is not a trivial task since the fast timescale control variables must react in a very precise and prompt fashion for the accurate tracking of the slow timescale pseudocontrols. The aileron roll is realized by constraining the bank angle μ as follows:

$$\mu_{\mathrm{DES}} = 0 \text{ deg}, \qquad t \le 1 \text{ s}$$
$$\mu_{\mathrm{DES}} = 180\{1 - \cos[2\pi(t-1)/10]\} \text{ deg}, \qquad 1 < t < 11 \text{ s}$$
$$\mu_{\mathrm{DES}} = 360 \text{ deg}, \qquad t \ge 11 \text{ s}$$

Because there are four unknowns for the slow timescale problem, namely $\bar{\alpha}$, $\bar{\beta}$, $\bar{\mu}$, and δ_T and, consequently, three degrees of redundancy, a cost function $S = 100(V - V_e)^2 + \chi^2 + \gamma^2$ is introduced,

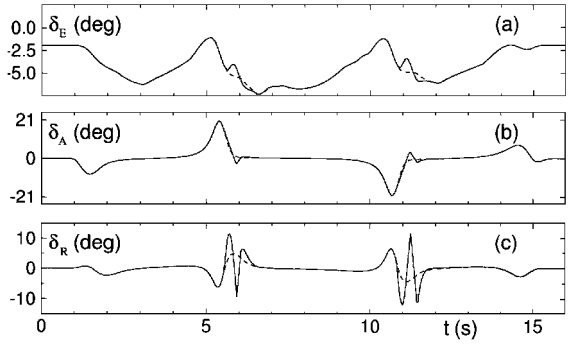

Fig. 5 Sequence of turns in the horizontal plane, effect of control saturation, $\Delta t = \frac{1}{4}$ s, $\delta t = \frac{1}{32}$ s: ——, rate and amplitude limited controls, and – – –, no limits on rate and amplitude.

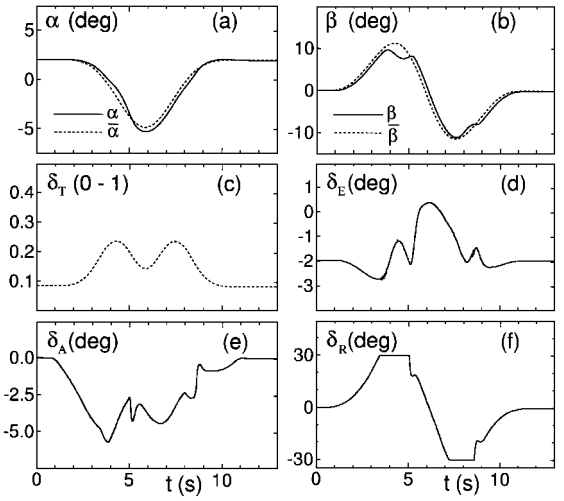

Fig. 6 Aileron roll, $\Delta t = \frac{1}{4}$ s, and $\delta t = \frac{1}{32}$ s.

where $V_e = 154$ ms^{-1}, and the angles are in degrees. The inverse problem is solved with the usual $\Delta t = \frac{1}{4}$ s and $\delta t = \frac{1}{32}$ s. Figure 6 shows the results for this maneuver. Note the saturation of the rudder angle in Fig. 6f at $t = 3.4$ and 7.1 s. This circumstance is responsible for the difference between the desired and achieved values of the pseudocontrols $\bar{\alpha}$ and $\bar{\beta}$ visible in Figs. 6a and 6b. The computed velocity V and the bank μ and roll angle ϕ are not shown as they present negligible variations from the desired values. The displacement of the achieved flight path from the straight line is as low as 4 m at the end of the maneuver.

V. Conclusions

In this paper a two-timescale procedure for the inverse simulation is presented. The methodology relies on the integration approach and eliminates some disadvantages and limitations of that technique, where the partial differentiation of output variables with respect to control inputs is often a critical task when systems with multiple timescales and right half-plane transmission zeros are dealt with.

The presented results show that the method allows for a substantial reduction of computer time in comparison with existing integration techniques while maintaining good characteristics of numerical accuracy and robustness. Control saturation is accounted for at either the slow or fast timescales, and the situations where the number of controls exceeds the number of constrained variables are very efficiently dealt with by assigning proper performance indexes in only one or both timescales, depending on the aircraft model and the simulated maneuvers.

As a final observation, we remark that the timescale separation eliminates unwanted effects on the numerical stability of the inverse simulation algorithm associated with the static instability of the model. Such effects, in some circumstances, prevent the application of integration techniques to baseline models of high performance aircraft where, to analyze the maximum performances of the basic, aerodynamic configuration of the vehicle, the stability and control augmentation system is not featured.

Acknowledgments

This work was partially supported by the Italian National Research Council through Contract N. 96.00049.74 and by the National Program of Researches in Antarctica.

References

[1]Kato, O., and Sugiura, I., "An Interpretation of Airplane General Motion and Control as Inverse Problem," *Journal of Guidance, Control, and Dynamics*, Vol. 9, No. 2, 1986, pp. 198–204.

[2]Ashley, H., "On the Feasibility of Low-Speed Aircraft Maneuvers Involving Extreme Angles of Attack," *Journal of Fluids and Structures*, Vol. 1, No. 3, 1987, pp. 319–335.

[3]Thomson, G. D., "Evaluation of Helicopter Agility Through Inverse Solution of the Equations of Motion," Ph.D. Thesis, Faculty of Engineering, Univ. of Glasgow, Scotland, UK, May 1987.

[4]Whalley, M. S., "Development and Evaluation of an Inverse Solution Technique for Studying Helicopter Maneuverability and Agility," NASA TM-102889, July 1991.

[5]Thomson, D. G., and Bradley, R., "The Use of Inverse Simulation for Preliminary Assessment of Helicopter Handling Qualities," *The Aeronautical Journal*, Vol. 101, No. 1007, 1997, pp. 287–294.

[6]Avanzini, G., de Matteis, G., de Socio, L. M., "Analysis of Aircraft Agility on Maximum Performance Maneuvers," *Journal of Aircraft*, Vol. 35, No. 4, 1998, pp. 529–535.

[7]Hess, R. A., and Gao, C., "A Generalized Algorithm for Inverse Simulation Applied to Helicopter Maneuvering Flight," *Journal of the American Helicopter Society*, Vol. 38, No. 4, 1993, pp. 3–15.

[8]Sentoh, E., and Bryson, A. E., "Inverse and Optimal Control for Desired Outputs," *Journal of Guidance, Control, and Dynamics*, Vol. 15, No. 3, 1992, pp. 687–691.

[9]Boyle, D., and Chamitoff, G., "Autonomous Maneuver Tracking for Self-Piloted Vehicles," *Journal of Guidance, Control, and Dynamics*, Vol. 22, No. 1, 1999, pp. 58–67.

[10]Heiges, M. W., Menon, P. K. A., and Schrage, D. P., "Synthesis of a Helicopter Full-Authority Controller," *Journal of Guidance, Control, and Dynamics*, Vol. 15, No. 1, 1992, pp. 222–227.

[11]Snell, S. A., Enns, D. F., and Garrard, W. L., "Nonlinear Inversion Control for a Supermaneuverable Aircraft," *Journal of Guidance, Control, and Dynamics*, Vol. 15, No. 4, 1992, pp. 976–984.

[12]Stiharu-Alexe, I., and O'Shea, J., "Four-Dimensional Guidance of Atmospheric Vehicles," *Journal of Guidance, Control, and Dynamics*, Vol. 19, No. 1, 1996, pp. 113–122.

[13]Avanzini, G., de Matteis, G., and de Socio, L. M., "Natural Description of Aircraft Motion," *Journal of Guidance, Control, and Dynamics*, Vol. 21, No. 2, 1998, pp. 229–233.

[14]de Matteis, G., de Socio, L. M., and Leonessa, A., "Solution of Aircraft Inverse Problems by Local Optimization," *Journal of Guidance, Control, and Dynamics*, Vol. 18, No. 3, 1995, pp. 567–571.

[15]Lee, S., and Kim, Y., "Time-Domain Finite Element Method for Inverse Problem of Aircraft Maneuvers," *Journal of Guidance, Control, and Dynamics*, Vol. 20, No. 1, 1997, pp. 97–103.

[16]Rutheford, S., and Thomson, D. G., "Improved Methodology for Inverse Simulation," *Aeronautical Journal*, Vol. 100, No. 993, 1996, pp. 79–86.

[17]Hess, R. A., Gao, C., and Wang, H. S., "Generalized Technique for Inverse Simulation Applied to Aircraft Maneuvers," *Journal of Guidance, Control, and Dynamics*, Vol. 14, No. 5, 1991, pp. 920–926.

[18]Lin, K.-C., "Comment on 'Generalized Technique for Inverse Simulation Applied to Aircraft Maneuvers,'" *Journal of Guidance, Control, and Dynamics*, Vol. 16, No. 6, 1993, pp. 1196, 1197.

[19]Yip, K. M., and Leng, G., "Stability Analysis for Inverse Simulation of Aircraft," *The Aeronautical Journal*, Vol. 102, No. 1016, 1998, pp. 345–351.

[20]Kepr, B., "Differential Geometry," *Survey of Applicable Mathematics*, edited by K. Rektorys, MIT Press, Cambridge, MA, 1969, pp. 306–317.

[21]Stevens, B. L., and Lewis, F. L., *Aircraft Control and Simulation*, Wiley, New York, 1992.

[22]Nguyen, L. T., Ogburn, M. E., Gilbert, W. P., Kibler, K. S., Brown, P. W., and Deal, P. L., "Simulator Study of Stall/Post-Stall Characteristics of a Fighter Airplane with Relaxed Longiudinal Static Stability," NASA TP-1538, 1979.